

Black-box data-driven computations of PDE solutions via network realizations of reduced order models

Vladimir Druskin

Worcester Polytechnic Institute and Brookline Advanced Algorithms Institute



Acknowledgments

- Contributors: Liliana Borcea, Leonid Knizhnerman, Alexander Mamonov, Shari Moskow, Mikhail Zaslavsky, Jörn Zimmerling
- This work was partially supported by AFOSR grants FA 955020-1-0079, FA9550-23-1-0220, and NSF grant DMS-2110773.

Outline

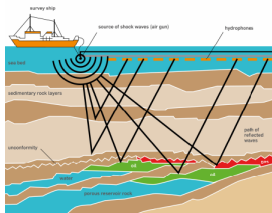
1 Motivations

2 Study case: 1D inverse impedance problem

- Stieltjes approximations, network synthesis view
- Finite-difference embedding on optimal grids
- Embedding of inverse problems via FD Gaussian quadratures
- Finite-difference computation of data-driven internal solutions
- Multidimensional formulation
- Non-overdetermined problem: SAR
 - Monostatic formulation
 - 2D example
- MIMO completion of SAR data

3 Conclusions

Inverse scattering problem



- To fix the idea, consider acoustic Helmholtz equation with appropriate boundary/infinity conditions in semiinfinite domain $\Omega \subset \mathbb{R}^3$ (e.g., lower half-space)

$$c^2(x)\Delta u(x, \lambda) + \lambda u(x, \lambda) = b(x),$$

with variable wavespeed $c(x)$. We can view this equation as the Laplace transformed wave or diffusion equations.

Other imaging applications

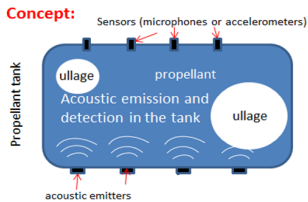


Figure: Gauging of propellant tanks in 0G for deep space exploration. Courtesy of Michael Khasin, NASA, Langley

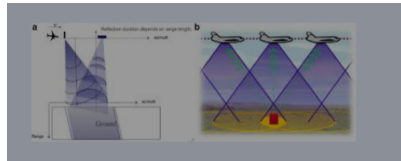


Figure: SAR in multiple scattering environment <https://www.sciencedirect.com/science/article/pii/S2468013319300622>

Model-ignorant data-driven PDE solutions

- Remote sensing data, black-box model
- Accurate estimate of the PDE solution at the inaccessible subdomain makes their imaging straightforward.
- Applications beyond imaging: Acoustic and electromagnetic focusing in medicine for tumor ablations

Model-ignorant data-driven PDE solutions. II

Objective

Estimation of the solution of LTI PDEs with unknown coefficients from their multiinput-multioutput (MIMO) transfer functions with small number of inputs (transmitters) and outputs (receivers).

Model-ignorant data-driven PDE solutions. II

Objective

Estimation of the solution of LTI PDEs with unknown coefficients from their multiinput-multioutput (MIMO) transfer functions with small number of inputs (transmitters) and outputs (receivers).

- Conventional ML approach requires massive data-sets for training: physically informed deep NN Karniadakis et al, 2019; shallow recurrent decoder networks for full-state reconstruction, Kutz et al 2023.
- We suggest an approach via network realizations of data-driven ROMs, requiring only a single training model.

Mathematicians enlisted to help us:



- From left to right: Thomas Joannes Stieltjes, 1856–1894; Wilhelm Cauer, 1900-1945; Mark Grigorievich Krein, 1907–1989; Israel Moiseevich Gelfand, 1913–2009.

Outline

1 Motivations

2 Study case: 1D inverse impedance problem

- Stieltjes approximations, network synthesis view
- Finite-difference embedding on optimal grids
- Embedding of inverse problems via FD Gaussian quadratures
- Finite-difference computation of data-driven internal solutions
- Multidimensional formulation
- Non-overdetermined problem: SAR
 - Monostatic formulation
 - 2D example
- MIMO completion of SAR data

3 Conclusions

1D inverse wave problem

- We consider a two-point 1D wave problem on $[0, L]$, $0 < L \leq \infty$ in the Laplace frequency domain,

$$-c(x)^2 \frac{d^2}{dx^2} u(x, \lambda) + \lambda u(x, \lambda) = 0, \quad \frac{d}{dx} u|_{x=0} = -1, \quad u|_{x=L} = 0,$$

where $c(x) > 0$ is variable wave-speed, in the Fourier domain $\lambda = -\omega^2$.

- We define impedance (a.k.a. NtD, Weyl or transfer) function as

$$f(\lambda) = u(x, \lambda)|_{x=0}.$$

- Inverse impedance problem

$$f(\lambda) \mapsto c(x).$$

Solvability, algorithms: Tikhonov, Marchenko, Gelfand, Levitan, Krein
1940s-1950s.

Stieltjes problems with discrete spectrum

- For $L < \infty$ the wave problem has discrete spectrum $\lambda_i > 0$,
 $i = 1, \dots, \infty$,

$$f(\lambda) = \sum_{i=1}^{\infty} \frac{c_i}{\lambda + \lambda_i}.$$

- The spectral decomposition yields $u = \sum_{j=1}^{\infty} \frac{z_j(0)z_j(x)}{s + \lambda_j}$, where z_j, λ_j are the eigenpairs of homogeneous problem (??) with normalization $\int_0^L \frac{z_j(x)^2}{c(x)^2} dx = 1$, so for the transfer function we obtain

$$u|_{x=0} = \sum_{j=1}^{\infty} \frac{z_j(0)^2}{s + \lambda_j}.$$

Pade approximants of transfer functions

- To **preserve structure** of the original problem consider Stieltjes rational approximants f_k of f , i.e.,

$$f_k(\lambda) = \sum_{i=1}^k \frac{y_i}{\lambda + \theta_i}$$

with negative non-coinciding poles θ_i and positive residues y_i .

- It is known, that the non-degenerate sub-diagonal $[k - 1, k]$ -Padé approximants of Stieltjes functions are also Stieltjes functions. They can be given by **$2k$ matching conditions**, e.g.:
 - Simple Padé approximation

$$\frac{d^i}{d\lambda^i}(f - f_k)|_{\lambda=s_0} = 0 \quad i = 0, \dots, 2k - 1, \quad (1)$$

where $s_0 \in]0, \infty[$ for $L = \infty$ and $s_0 \in [0, \infty[$ otherwise.

- Rational interpolation (a.k.a. multipoint Padé)

$$(f - f_k)|_{\lambda=s_i} = 0, \quad 0 < s_1 < \dots < s_{2k}. \quad (2)$$

Stieltjes continued fraction (S-fraction), hidden layers

Theorem (Thomas Joannes Stieltjes, 1893)

Any partial fraction $f_k(\lambda)$ with positive residues y_i and non-coinciding poles $-\theta_i \in \mathbb{R}_-$ can be equivalently presented as S-fraction

$$\sum_{i=1}^k \frac{y_i^2}{\lambda + \theta_i} = \cfrac{1}{\hat{h}_1 \lambda + \cfrac{1}{h_1 + \cfrac{1}{\hat{h}_2 \lambda + \dots \cfrac{1}{h_{k-1} + \cfrac{1}{\hat{h}_k \lambda + \frac{1}{h_k}}}}}}$$

with real positive coefficients $\hat{h}_i, h_i, i = 1, \dots, k$ via a $O(k)$ direct algorithm (e.g., Lanczos).

Stieltjes discrete inversion algorithm ¹

- We set $\vartheta_{2i-1} = \sqrt{\theta_i}$, $\vartheta_{2i} = -\sqrt{\theta_i}$, $i = 1, \dots, k$ and initialize

$$w_{2i-1}^1 = \sqrt{0.5y_i}, \quad w_{2i}^1 = \sqrt{0.5y_i}, \quad \hat{w}_{2i-1}^0 = 0, \quad \hat{w}_{2i}^0 = 0, \quad i = 1, \dots, k.$$

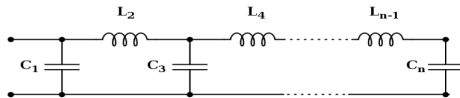
Then $\hat{\gamma}_j, \gamma_j$ are found via steps 1 through 4 repeated recursively for $j = 1, \dots, k$

- ① $\hat{\gamma}_j = \frac{1}{\sum_{i=1}^{2k} (w_i^j)^2},$
- ② for $i = 1, \dots, 2k$
 - $\hat{w}_i^j = \hat{w}_i^{j-1} + \hat{\gamma}_j \vartheta_i w_i^j,$
- ③ $\gamma_j = \frac{1}{\sum_{i=1}^{2k} (\hat{w}_i^j)^2},$
- ④ for $i = 1, \dots, 2k$
 - $w_i^{j+1} = \hat{w}_i^j + \gamma_j \vartheta_i \hat{w}_i^j,$

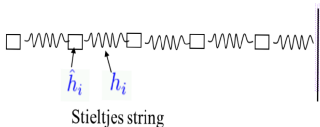
¹A. k. a.: (first order) polynomial orthogonalization recursion; Lanczos alg.; Euclidean alg.; Jacobi inverse eigenvalue method; discrete Marchenko-Krein-Gelfand-Levitan alg.; finite-difference layer stripping.

Cauer LC filter synthesis interpretation

- Impedance $f_k(\lambda)$ is the impedance of LC network with $\lambda = -\omega^2$,
 $\hat{\gamma}_i = C_i$, $\gamma_i = L_i^{-2}$



- Mechanic interpretation as a (Stieltjes) string of weightless springs with stiffness $\gamma_i = h_i$ and point masses $\hat{\gamma}_i = \hat{h}_i$ is due to Mark Krein, 1950:



²Cauer, W, "Die Verwirklichung der Wechselstromwiderstände vorgeschriebener Frequenzabhängigkeit", Archiv für Elektrotechnik, vol 17, pp355–388, 1926. The realisation of impedances of prescribed frequency dependence (in German)

ROM interpretation

- Equivalently, we can rewrite the Stieltjes string as a ROM realization in the form

$$f_k(\lambda) = \frac{1}{\hat{\gamma}_1} \mathbf{e}_1^T (\mathcal{T} + \lambda I)^{-1} \mathbf{e}_1,$$

where

$$\mathcal{T} = \begin{pmatrix} \alpha_1 & \beta_1 & 0 & \dots & & 0 \\ -\beta_1 & \alpha_2 & \beta_2 & 0 & \dots & 0 \\ & & \ddots & & & \\ 0 & \dots & 0 & \beta_{k-2} & \alpha_{k-1} & \beta_{k-1} \\ 0 & & \dots & 0 & -\beta_{k-1} & \alpha_k \end{pmatrix}$$

with $\alpha_i = -\hat{\gamma}_i^{-1/2} \left(\frac{1}{\gamma_{i-1}} + \frac{1}{\gamma_i} \right) \hat{\gamma}_i^{-1/2}$, (assuming $\frac{1}{\gamma_0} = 0$), and
 $\beta_i = \frac{1}{\gamma_i \sqrt{\hat{\gamma}_i \hat{\gamma}_{i+1}}}.$



Decoding data via ladder network?

PDE coefficients are encoded in the data, which we transform to the coefficients of an equivalent network. Can this transformation serve as a partial decoding of the data-generating model?

Finite-difference interpretation

- The ladder LC dynamical system can be written in finite-difference form as

$$f_k = w_1,$$

where w_1 is Dirichlet component of the finite-difference solution

$$\begin{aligned} \frac{1}{\hat{\gamma}_i} \left(\frac{w_{i+1} - w_i}{\gamma_i} - \frac{w_i - w_{i-1}}{\gamma_{i-1}} \right) - \lambda w_i &= 0, \quad i = 1, \dots, k, \\ \left(\frac{w_2 - w_1}{\gamma_1} \right) - \hat{\gamma}_1 \lambda w_1 &= 1, \quad w_{k+1} = 0. \end{aligned}$$

- When $c(x) \equiv 1$ the Stieltjes parameters can be interpreted as primary and dual steps of a finite-difference grid³, i.e., $h_i = \gamma_i$, $\hat{h}_i = \hat{\gamma}_i$:



³FD Gaussian Quadratures aka Optimal Grids, Dr.&Knizhnerman, SINUM, 1999

Examples of FD Gaussian rules, $k = 10$

0	*** * * * * * * * * *	1
---	-----------------------	---

Padé for $L = 1$, exponential convergence.⁴

0	*** * * * * * * * * *	1
---	-----------------------	---

Multipole Padé with Zolotarev parameters for $L = \infty$, optimal exponential convergence for a prescribed spectral interval.⁵ Used for optimal PML discretization.⁶

⁴Dr.&Knizhnerman, SINUM 2000

⁵Ingerman, Dr., Knizhnerman, Comm. Pure&Appl. Math., 2000

⁶Dr.,Guettel,Knizhnerman, SIREV 2016

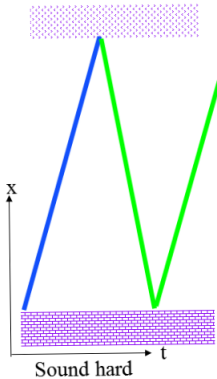
Embedding for 1D wave problem. I

Example: plane wave propagation

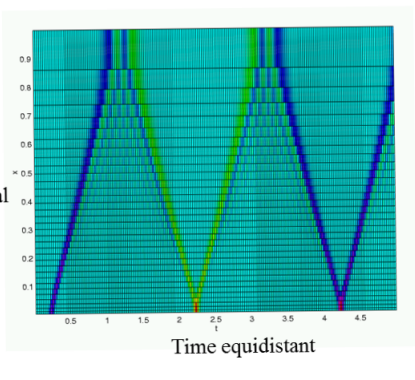
$$u_{xx} - u_{tt} = 0;$$

$$u_x|_{x=0} = g(t), \quad u|_{x=1} = 0; \quad u|_{t<0} = 0.$$

Sound soft



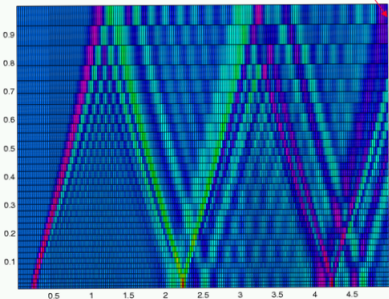
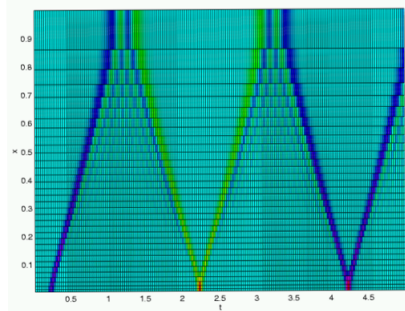
Space
optimal



Time equidistant

Embedding for 1D wave problem. II

Example: 1D wave propagation
optimal grid + 1 node



Finite-difference inverse problem

- The solution of the inverse problem can be simplified, if the FD Gaussian quadrature is **weakly** dependent on variations of $c(x)$.
- Weak dependence (more precisely, asymptotic independence) can be achieved after transformation to the travel time coordinates⁷
 $dT = \frac{dx}{c(x)}$ yielding

$$-\frac{d}{dT} \left(\frac{1}{c(T)} \frac{d}{dT} u(x, \lambda) \right) + \frac{\lambda}{c(T)} u(T, \lambda) = 0$$

- That gives finite difference coefficients $\gamma_i = h_i c_i$, $\hat{\gamma}_i = \frac{\hat{h}_i}{\hat{c}_i}$, where c_i and \hat{c}_i as finite-difference $c(x)$ defined at resp. primary and dual grid nodes.

⁷Borcea, Dr., Knizhnerman, CPAM, 2005.

Inversion examples

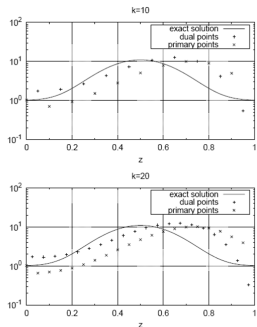


FIGURE 4.2. Inversion for the Gaussian bell $\sigma(z) = 1 + 10 \exp[-25(z - 0.5)^2]$, with TM data, on equidistant grids with 10 and 20 nodes.

Figure: Equidistant grid

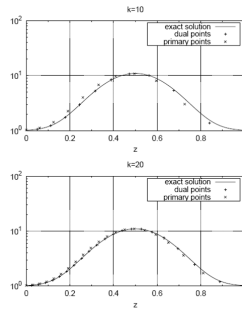


FIGURE 4.1. Inversion for the Gaussian bell $\sigma(z) = 1 + 10 \exp[-25(z - 0.5)^2]$, with TM data, on optimal grids \mathcal{G}_{10}^0 and \mathcal{G}_{20}^0 .

Figure: Optimal grid

Convergence result

We assume that training and measured (validation) data are computed by matching first k terms of the partial fraction expansions of corresponding transfer functions.

Theorem (Borcea et al, CPAM 2005)

Let us (for simplicity) assume, that the he finite-difference Gaussian quadrature is computed for $c(T) \equiv 1$. Then \forall uniformly positive and bounded $c(T)$, $c(T) \in H^3$ discrete c_i and \hat{c}_i converge to the true $c(T)$ at the FD nodes iff the FD grid is asymptotically close to the finite-difference Gaussian quadrature as $k \rightarrow \infty$.

Corollary

The FD Gaussian quadratures for all uniformly positive and bounded $c(T)$, $c(T) \in H^3$ asymptotically close to each other as $k \rightarrow \infty$

Embedding the data-driven finite-difference approximation

- The FD grid in travel-time coordinates T for large k asymptotically does not depend on $c(T)$ \Rightarrow the solution can be computed by just solving the data driven network problem

$$\frac{1}{\hat{\gamma}_i} \left(\frac{u_{i+1} - u_i}{\gamma_i} - \frac{u_i - u_{i-1}}{\gamma_{i-1}} \right) - \lambda u_i = 0, \quad i = 1, \dots, k,$$

$$\left(\frac{u_1 - u_0}{\gamma_0} \right) = -1, \quad u_{k+1} = 0$$

using the grid computed as the FD Gaussian quadrature for a known background model - **a single training model!**

- The data-driven network embedding using the FD Gaussian quadratures gives spectral convergence of $f(\lambda)$ but only second order in the interior for the best case scenario. Can we achieve better convergence?

Galerkin equivalent

- Let $(f_k - f)|_{\lambda=\lambda_i} = 0, \quad \frac{d}{d\lambda}(f_k - f)|_{\lambda=\lambda_i} = 0, \quad i = 1, \dots, k.$

f_k can be equivalently obtained as the Galerkin projection on the snapshot subspace $U = \text{span}\{u(x, \lambda_1), \dots, u(x, \lambda_k)\}$ ⁸

The ladder LC network is equivalent to the Galerkin projection on the snapshot subspace using a data-driven pivoted QR orthogonalized basis $v_i(x)$ ⁹, i.e. the Galerkin approximation $u(x, \lambda) \in U$ can be presented as

$$u(x, \lambda) \approx u(x, \lambda) = \sum_{i=1}^k w_i(\lambda) v_i(x),$$

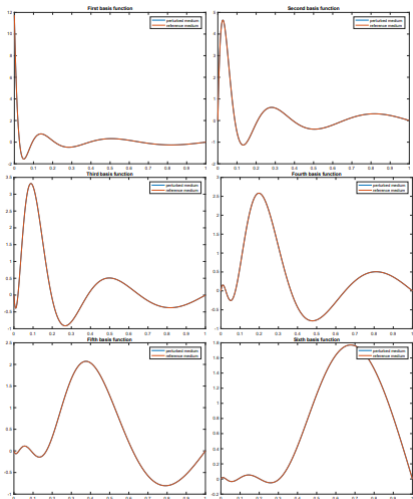
where w_i are the solutions on the data-driven network.

- Recall that $w_i(\lambda) \approx u(x, \lambda)$, i.e. $v_i(x)$ is similar to a nodal FE basis, thus tri-diagonal Galerkin matrix.

⁸Interpolatory projection method, Antoulas, Beattie, Gugercin, 2007

⁹Borcea, V Druskin, A Mamonov, S Moskow, M Zaslavsky, Inverse Problems, 2020

Basis $v_i(x)$, example with $k = 6$



- Basis $v_i(x)$ is peaked at the nodes of the FD Gaussian quadrature

Data-driven internal solutions

- Difference between background $u_0(x, \lambda)$ and internal solution $u(x, \lambda)$ can be large for large enough perturbations $\|c - c_0\|$, however the difference between (known) background basis functions $v_i(x)_0$ and their (unknown) internal counterparts $v_i(x)$ remains small, so we obtain formula of the data-driven internal solutions (DDIS)
$$u(x, \lambda) \approx \sum_{i=1}^k w_i(\lambda) v_i(x)_0.$$

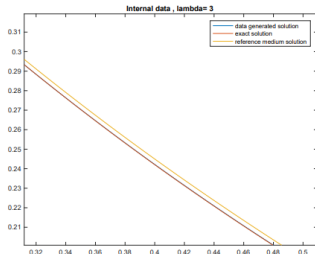


Figure: Data-driven internal solution in Laplace domain

Time domain example, modulated Gaussian pulse

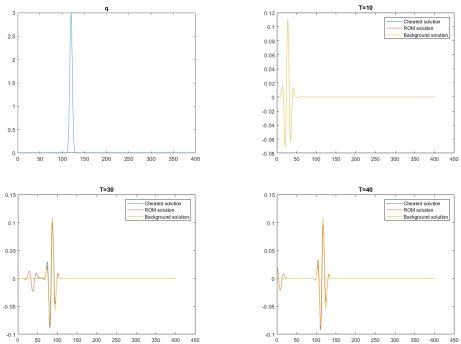


Figure: Reflectivity (Schrodinger potential) $q = \frac{\sqrt{c(T)}_{TT}}{\sqrt{c(T)}}$ (top left) and data generated internal snapshots (other plots). Before hitting the reflector, all overlap. After that, the DDIS show reflections very close to the true ones, however the background solutions do not show any reflections.

Block-generalization

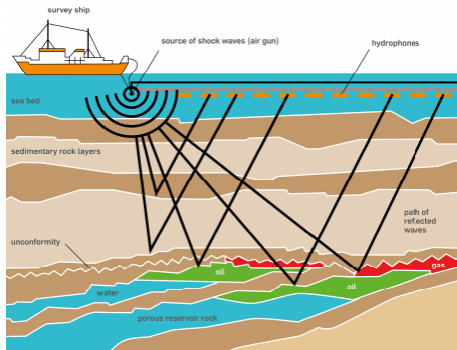
- All SISO linear algebra is automatically extended to the MIMO case with transfer function $F(t) \in \mathbb{R}^{m \times m}$ by using $m \times m$ matrices instead of numbers, i.e., instead of tridiagonal $\mathcal{T} \in \mathbb{R}^{n \times n}$ we will have block-tridiagonal matrix $\mathbb{T} \in \mathbb{R}^{mn \times mn}$ with $m \times m$ blocks.
- Blocks of \mathbb{T} are full, so we consider semi-discrete Galerkin interpretation, with localized "elements", i.e., solution of the problem

$$\begin{aligned} \mathbb{T}w - w_{tt} &= 0 \\ w|_{t=0} = e_1, \quad w_t|_{t=0} = 0, \quad \left(\frac{w_1 - w_0}{\gamma_0} \right) &= 0, \quad w_{k+1} = 0 \end{aligned}$$

gives decomposition with respect to the Galerkin elements.

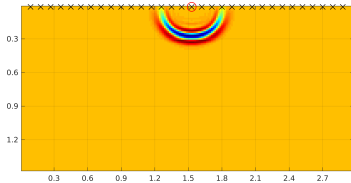
- Critically important: the the Galerkin elements almost independent on model reflectivity (in dominant travel-times coordinates), so one can use the elements for homogeneous background.

Seismic problem

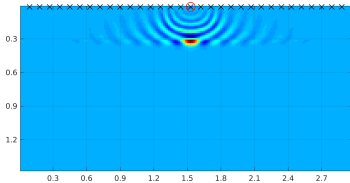


Localized 2D elements

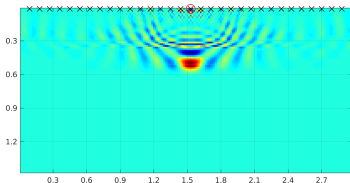
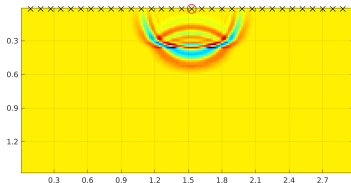
Internal solution



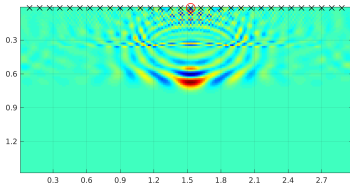
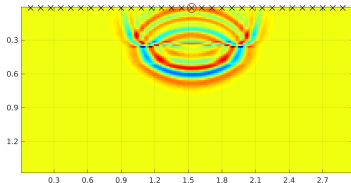
Elements



$t = 10\tau$



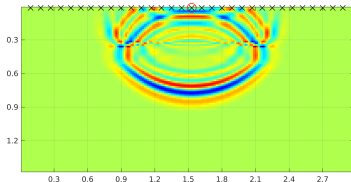
$t = 15\tau$



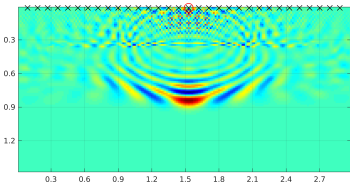
$t = 20\tau$

Localized 2D elements

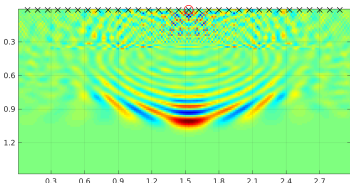
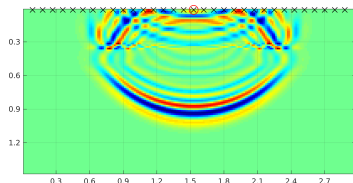
Snapshots



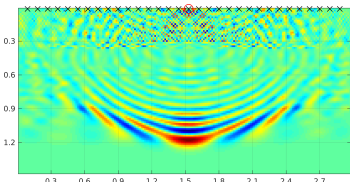
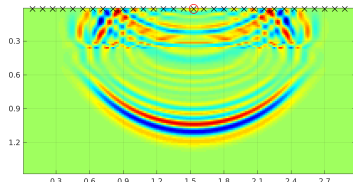
Elements



$t = 25\tau$



$t = 30\tau$



$t = 35\tau$

Almost model independent smile

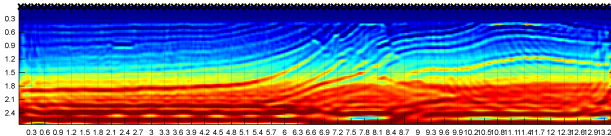
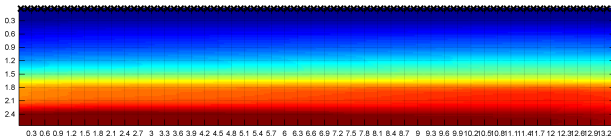
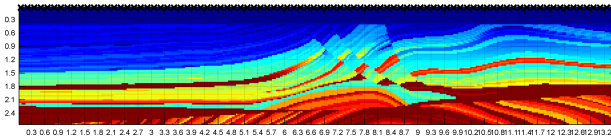


- The 2D orthogonalized snapshots V are localized ‘smiles’, weakly depend on the model in the coordinates aligned with the slowness surfaces of waves similar to the 1D case.
- Then data-driven internal solution (DDIS) is computed as

$$u \approx V_0 w,$$

where w is the Galerkin projection computed from the data, V_0 are the smile space computed from the known background $c_0(T)$.

Large scale model: 2D Marmousi; 1D background



From top to bottom: 2D Marmousi model (section); background (1D model); image.

Multidimensional generalizations

- The transient data-driven ROM approach is extendable to multidimensional MIMO problems with $\mathbb{R}^{2d-2} \times t$ DtN maps for problems in \mathbb{R}^d by using block (tensor) formulations.

- [1] L. BORCEA, V. DRUSKIN, AND L. KNIZHNERMAN, *On the continuum limit of a discrete inverse spectral problem on optimal finite difference grids*, Communications on Pure and Applied Mathematics, 58 (2005), pp. 1231–1279.
- [2] L. BORCEA, V. DRUSKIN, A. MAMONOV, S. MOSKOW, AND M. ZASLAVSKY, *Reduced order models for spectral domain inversion: embedding into the continuous problem and generation of internal data*, Inverse Problems, 36 (2020), p. 055010.
- [3] L. BORCEA, V. DRUSKIN, A. V. MAMONOV, AND M. ZASLAVSKY, *Robust nonlinear processing of active array data in inverse scattering via truncated reduced order models*, Journal of Computational Physics, 381 (2019), pp. 1–26.
- [4] L. BORCEA, J. GARNIER, A. V. MAMONOV, AND J. ZIMMERLING, *Waveform inversion with a data driven estimate of the internal wave*, arXiv, (2022).
- [5] L. BORCEA, J. GARNIER, A. V. MAMONOV, AND J. T. ZIMMERLING, *Waveform inversion via reduced order modeling*, ArXiv, abs/2202.01824 (2022).
- [6] V. DRUSKIN, A. V. MAMONOV, A. E. THALER, AND M. ZASLAVSKY, *Direct, nonlinear inversion algorithm for hyperbolic problems via projection-based model reduction*, SIAM Journal on Imaging Sciences, 9 (2016), pp. 684–747.
- [7] V. DRUSKIN, A. V. MAMONOV, AND M. ZASLAVSKY, *A nonlinear method for imaging with acoustic waves via reduced order model backprojection*, SIAM Journal on Imaging Sciences, 11 (2018), pp. 164–196.
- [8] V. DRUSKIN, S. MOSKOW, AND M. ZASLAVSKY, *Lippmann–schwinger–lanczos algorithm for inverse scattering problems*, Inverse Problems, 37 (2021), p. 075003.

Synthetic aperture radar (SAR) imaging

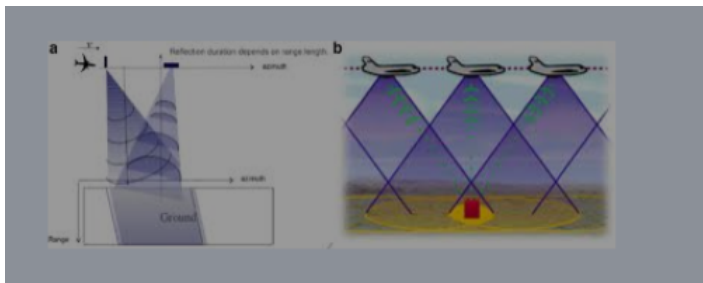


Figure: <https://www.sciencedirect.com/science/article/pii/S2468013319300622>

- Mono-static radar measurements along flight path (or several paths) are combined for imaging.
- Linear processing, e.g., the RTM or Born inversion: ⇒ **Significant nonlinear artifacts in multiple scattering environments are possible.**

Dimensional consistency of SAR data

- At every monostatic location SAR collect function of time ⇒
 - 2D data set for one flight path → 2D inverse problem
 - Multiple flight paths covering a surface region yield 3D data sets → 3D inverse problem
- Born inversion can be reduced to classical integral geometry problems, e.g., *Lavrent'ev, Romanov, Vasiliev, Multidimensional inverse problems for differential equations, Lecture Notes in Mathematics, Vol. 167, Springer-Verlag, Berlin, 1970; Fawcett, Inversion of N-Dimensional Spherical Averages, SIAM Journal on Applied Mathematics, Vol. 45, N. 2 (1985)*

Synthetic aperture radar (SAR) setup

- Consider scalar approximation of electromagnetic wave scattering

$$Au^{(T)} + u_{tt}^{(T)} = 0, \quad u_t|_{t=0} = 0, \quad u|_{t=0} = b^{(T)},$$

with Schödinger operator $Au = -\Delta u + q(x)u$, $x \in \mathbb{R}^s$, $s = 2, 3$.

- Monostatic formulation, transmitter coincides with receiver:

$$f^{(T)}(t) = \int_{\mathbb{R}^s} u^{(T)}(x, t) b^{(T)}(x) d^s x.$$

- SAR: data are given by trajectory $x'(T)$ of the monostatic transmitter/receiver

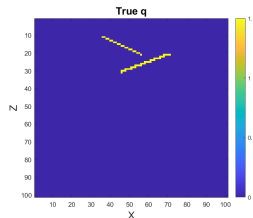
$$b^{(T)} \approx \delta(x - x'(T)),$$

where T is assumed much slower than t .

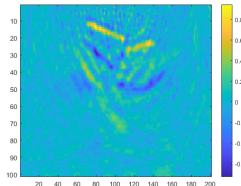
Asymptotic properties of monostatic formulation

- For a proper full square MIMO setup the data-driven formula for the internal field remains valid
- In contrast, the monostatic setup does not provide enough functions in the subspace to cancel all of the reflections from different directions during orthogonalization \Rightarrow not enough information for accurate data-driven solutions.
- The data for different T are coupled via corresponding LS equations.

Two reflectors 2D example



True model



Born image

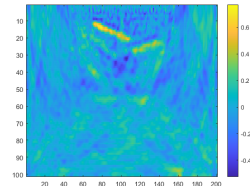


Image with DDIS

- The SAR data is obscured by multiple echoes
- We image the reflectivity distribution to map the boundaries of the reflectors from the SAR data
- 2.5D inversion (3D waves scattered by 2D reflectors) results are available in [Dr., Moskow, Zaslavsky, 2022]

SAR vs MIMO for multidimensional settings

- The straight-forward DDIS approach with SAR data only partially suppress multiple reflections, not enough to suppress multi-path arrivals. The block approach with MIMO transfer function of sufficient aperture suppress those arrivals.
- The SAR data is the diagonal of the square MIMO matrix transfer function. The latter is necessary for the block approach. How to estimate off-diagonal elements from the diagonal of the s.p.d. data matrix?

Lifting SAR to MIMO

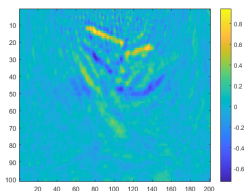
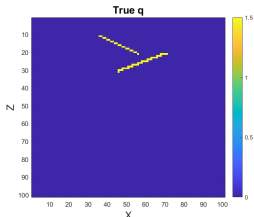
- Let T_1, \dots, T_n is a discretization of the SAR trajectory. We denote the (unavailable) MIMO data set as f^{T_i, T_j} with the measured SAR data set $f^{T_i, T_i} = f^{T_i}$
- Matrix completion problem:¹⁰ Born postprocessing of the SAR LSL inversion for the off-diagonal elements. Trick: structure preserving by spectral correction of the data-driven Gramian M

$$(f^{T_1, T_1}, \dots, f^{T_n, T_n}) \Rightarrow \begin{bmatrix} f^{T_1, T_1} & f^{T_1, T_2} & \cdot & f^{T_1, T_n} \\ f^{T_2, T_1} & f^{T_2, T_2} & \cdot & f^{T_2, T_n} \\ \cdot & \cdot & \ddots & \cdot \\ f^{T_n, T_1} & \cdot & \cdot & f^{T_n, T_n} \end{bmatrix}$$

- The transformation is very close to linear. In principle, can be done recursively, however one step is sufficient in our examples.

¹⁰Dr.,Moskow,Zaslavskiy, 2023, in preparation

Two reflectors 2D example, LSL with data completion



Born image

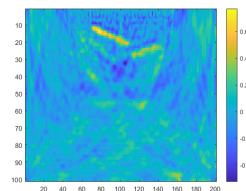


Image with DDIS

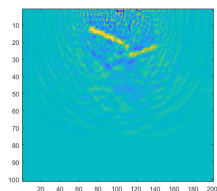


Image with completed DDIS

- The SAR data is obscured by multiple echoes.
- Using DDIS partially removes nonlinear artifacts on SAR images
- DDIS + data completion further improves quality of the SAR image

Outline

1 Motivations

2 Study case: 1D inverse impedance problem

- Stieltjes approximations, network synthesis view
- Finite-difference embedding on optimal grids
- Embedding of inverse problems via FD Gaussian quadratures
- Finite-difference computation of data-driven internal solutions
- Multidimensional formulation
- Non-overdetermined problem: SAR
 - Monostatic formulation
 - 2D example
- MIMO completion of SAR data

3 Conclusions

Summary

- Embedding network realizations of data-driven reduced order model allows to compute the state solutions from the sufficient set of remote MIMO measurements only using only one training model.
- There some issues in the case of the severely restricted measurements, such as SAR when data-completion is needed.
- We showed applications in seismic imaging and SAR
- Potential applications in radar imaging and other active array formulations, e.g., seismic, control source electromagnetic exploration, nondestructive testing, medical imaging (ultrasound) and focused medical treatments of the interior tissues
- Not in this talk:
 - Other applications for full wave inversion in seismic exploration and imaging in random media, e.g., [Borcea, Garnier, Mamonov, Zimmerling, 2022].
 - Imaging in lossy media via damped strings [Borcea, Dr., Zimmerling, Sc.Comp. 2021], [Zimmerling, Dr., Cherkaev, Guddati, Remis, 2023]
 - Imaging and gauging of propellant tanks in 0-G, Baker, Cherkaev, Moskow, Druskin, Zaslavskiy, in preparation.